Available online at www.sciencedirect.com
ScienceDirect
Geochimica et Cosmochimica Acta 70 (2006) 5236–5245
Geochimica
www.elsevier.com/locate/gca

Experimental constraints on the mobility of Rhenium in silicate liquids

Jason M. MacKenzie *, Dante Canil

School of Earth and Ocean Sciences, University of Victoria, Victoria, BC, Canada V8W 3P6

Received 27 October 2005; accepted in revised form 31 July 2006

Abstract

The volatization of Rhenium (Re) from melts of natural basalt, dacite and a synthetic composition in the CaO–MgO–Al_2O_3–SiO_2 system has been investigated at 0.1 MPa and 1250–1350 °C over a range of fO_2 conditions from $\log fO_2 = -10$ to -0.68. Experiments were conducted using open top Pt crucibles doped with Re and Yb. Analysis of quenched glasses by laser ablation-inductively coupled plasma mass spectrometry (LA-ICP-MS) normal to the melt/gas interface showed concentration profiles for Re, to which a semi-infinite one-dimensional diffusion model could be applied to extract diffusion coefficients (D). The results show Re diffusivity in basalt at 1300 °C in air is $\log D_{Re} = -7.2 \pm 0.3$ cm^2/s and increases to $\log D_{Re} = -6.6 \pm 0.3$ cm^2/s when trace amounts of Cl were added to the starting material. At fO_2 conditions below the nickel–nickel oxide (NNO) buffer Re diffusivity decreases to $\log D_{Re}^{reducing} = -7.6 \pm 0.2$ cm^2/s and to $\log D_{Re}^{dacite} = -8.4 \pm 0.2$ cm^2/s in dacitic melt. In the CMAS composition, $\log D_{Re}^{CMAS} = -7.5 \pm 0.1$. The diffusivity of Re is comparable to Ar and CO_2 in basalt at 500 MPa favoring its release as a volatile. Our results support the contention that subaerial degassing is the cause of lower Re concentrations in arc-type and ocean island basalts compared to mid-ocean ridge basalts.

1. Introduction

Rhenium is a moderately incompatible element whereas Osmium is a highly compatible element retained in the mantle during melt extraction to form the crust (Shirey and Walker, 1998). These unique geochemical properties highlight the utility of the Re–Os isotopic system in studies of magma genesis (Righter and Hauri, 1998), crustal recycling (Becker, 2000; Sun et al., 2003a) and mantle evolution (Brenan et al., 2003).

The Earth's major geochemical reservoirs include mid-ocean ridge basalts (MORBs) depleted MORB mantle, continental crust and the primitive mantle. Constraints regarding Re and Os abundances and isotopic ratios in these reservoirs are continually evolving, but experimental data on the behavior of Re and Os at high P and T are limited, creating uncertainty to models for the distribution of these elements in the solid earth system. For example, in numerous geochemical studies, Re has been shown to exhibit a range of behaviors from volatile (Lassiter, 2003) and chalcophile (Alard et al., 2002), to siderophile and moderately incompatible lithophile (Righter and Hauri, 1998; Brenan et al., 2003; Sun et al., 2003a).

Sun et al. (2003a) suggested that the mantle–crust reservoirs are not balanced with respect to their Re contents and Re/lithophile-element ratios. Yb and Re are similarly incompatible during formation of MORB, as evidenced by their restricted Re contents [~0.926 ppb (Righter and Hauri, 1998) and Re/Yb ratios (~280 ppt/ppm) (Hauri and Hart, 1997)]. In the depleted MORB mantle however, Re is strongly depleted relative to Yb. A mass balance between continental crust, depleted MORB mantle and primitive mantle indicates that the crustal abundance of Re is too low to balance the Re depletion estimated for depleted MORB mantle (Hauri and Hart, 1997) creating a paradox for the processes responsible for Re depletion in the mantle-derived melts.

The Re contents of ocean–island basalts (OIB), arc-type basalts or MORB are governed by the behavior of this element in their mantle source region and its mobility during ascent and emplacement of magma. The average Re con-

* Corresponding author.
E-mail address: jasonmac@uvic.ca (J.M. MacKenzie).

0016-7037/$ - see front matter © 2006 Elsevier Inc. All rights reserved.
doi:10.1016/j.gca.2006.07.032

centrations in MORBs are 0.956 ± 0.349 ppb, considerably higher than in OIB (0.414 ± 0.235 ppb). The Re concentrations in arc-type basalts is generally lower (0.233 ± 0.170 ppb) than both MORB and OIB but varies significantly from <1 to 800 ppt (Woodhead and Brauns, 2004) (Fig. 1). The variability in the Re content of arc-type basalts could reflect complex interactions between melting and fluid release of subducted slabs and the overlying mantle wedge, or volatile release during the emplacement of arc magmas.

Righter and Hauri (1998) attributed differences in the Re contents between MORB and OIB to the presence of garnet in the mantle source of the latter magma type. In this model, the missing Re to balance the crustal and mantle reservoirs is retained in garnet residual from partial melting. Alard et al. (2002) found elevated concentrations of Re in residual sulphides in peridotite xenoliths hosted in alkali basalts. This observation suggests residual sulfide phase can serve as a sink for the missing Re between OIB and MORB, but not all magmas are necessarily sulphide-saturated at their source.

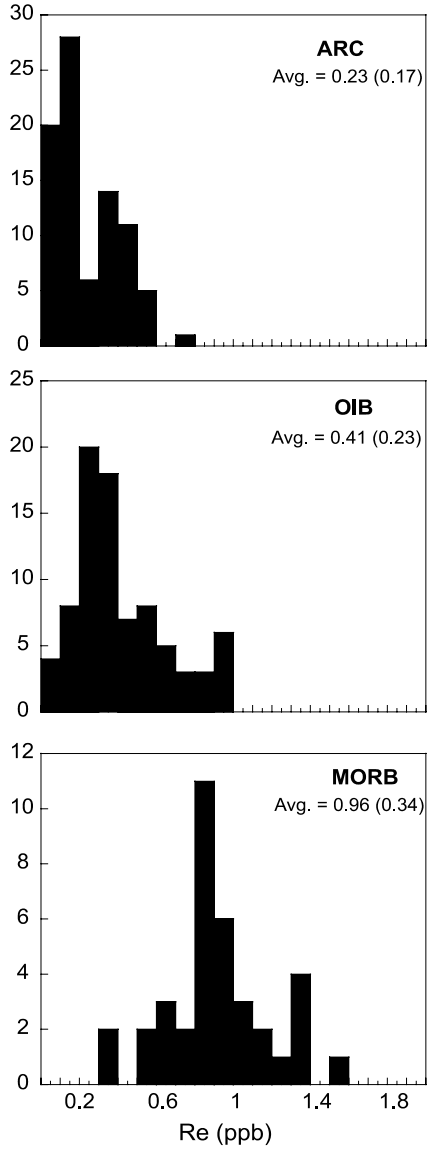

Fig. 1. Histogram of Re contents from MORB, OIB and arc-type basalts showing arithmetic mean and 1σ standard deviation in brackets. Data sources are: MORB—(Roy-Barman and Allègre, 1994; Schiano et al., 1997; Woodhead and Brauns, 2004), OIB—(Widom and Shirey, 1996; Hauri and Kurz, 1997; Lassiter and Hauri, 1998; Bennett et al., 2000; Schiano et al., 2001; Lassiter, 2003), ARC—(Alves et al., 1999; Borg et al., 2000; Alves et al., 2002; Chesley et al., 2002; Woodhead and Brauns, 2004).

Arc magmas are generally considered to be the major building blocks of continental crust (Sun et al., 2003a). As such, the Re contents of arc magmas should provide a good estimate of Re transfer from partial melting of the mantle to form the continental crust. Problematically, most Re analyses of arc magmas are from subaerially erupted samples (Lassiter, 2003; Sun et al., 2003a) which, if Re exhibits volatile behavior, could serve to underestimate their Re contents and the resulting the magnitude of Re transfer from the mantle to the continental crust.

There is convincing evidence that Re is volatile at volcanic edifices. Crowe et al. (1987) noted high Re concentrations in volcanic gasses from Kilauea volcano and established a Re flux of 2.4E-02 mg/m^3. Re enrichment and pure Re-sulphide condensates have been observed in fumaroles from Kudryavy (Korzhinsky et al., 1994; Taran et al., 1995). Lassiter (2003) measured Re concentrations in lava sequences from drill core from Mauna Loa and found lower Re levels in those lavas calculated to have erupted subaerially. Further quantification of Re volatility and degassing from volcanic edifices requires knowledge of the behavior of Re in silicate liquids and its partitioning and transport behavior to and across melt/gas interfaces. Towards this end, the goal of this study is to measure the diffusivity of Re as a volatile element from silicate liquids as well as to establish the role of intensive variables [i.e., melt composition (X), T and fO_2] that control its mobility.

2. Experimental

2.1. Experimental methods

To measure diffusion rates, we used Re-doped melts in contact with a gas phase. The technique uses the volatility of this element (Borisov and Jones, 1999) to establish a concentration gradient where Re in the melt must equilibrate with the atmosphere above it. The concentration gradients resulting from volatilization of Re were measured to investigate its chemical diffusivity in melts of different compositions and under different ambient fO_2 conditions. A similar experimental design was used to measure F diffusion in silicate liquids (Dingwell and Scarfe, 1985).

Starting materials were natural basalt (MIC99-8) from the Eocene Metchosin Igneous complex (Vancouver Island, BC), dacite (WP-1) from the Quaternary Watts Point lava dome (Squamish, BC) and a synthetic CaO–MgO–Al_2O_3–SiO_2 (CMAS) composition (Table 1). To prepare starting materials, basalt or dacite powder was ground in an agate

Table 1
Major and trace element concentration of starting materials

Sample	MIC99-8	MIC99-8 (+Cl)	WP-1	CMAS
Na_2O	2.3	2.7	3.5	—
MgO	8.1	8.0	2.6	10.8 (0.2)
Al_2O_3	15.0	14.9	16.6	15.4 (0.2)
SiO_2	48.1 (0.2)	48.0	64.7 (0.2)	49.1 (0.2)
P_2O_5	0.1	0.1	0.2	—
K_2O	0.1	0.1	1.7	—
CaO	12.2	12.2	5.0	24.6 (0.2)
TiO_2	1.1	1.1	0.5	—
MnO	0.2	0.2	0.1	—
Fe_2O_3	12.2	12.1	4.7 (0.2)	—
Cl	b.d.	b.d.	—	—
S	b.d.	b.d.	—	—
Re (ppm)	1.0 (0.15)	1.0 (0.15)	1.5 (0.1)	10.0 (0.5)
Total	99.3	99.4	99.5	99.9

Concentrations are averages of 20 measurements for the MIC99-8 (±Cl) and CMAS compositions. WP1 composition is average of 10 measurements. Measurements were made on randomly selected chips of start glass. 1σ standard deviation for major elements is ±0.1 wt% unless other wise noted in brackets. 1σ standard deviation for Re in starting glass are shown in brackets. MIC99-8 ($Fe^{3+}/Fe^{total} = 0.88$), WP-1 ($Fe^{3+}/Fe^{total} = 0.79$) (calculated after Kress and Carmichael, 1988) Detection limits for Cl and S are 500 and 350 ppm, respectively. All Fe reported Fe_2O_3, b.d. (below detection).

mortar and dried at 100 °C in air for 1 h. Once dried, 1000 ppm NIST certified Re standard solution was added to each powder using a micropipette. The powder and solution were subsequently ground under alcohol for 10 min to homogenize the mixture. After drying, the mixture was loaded into a 25 mm diameter Pt crucible and fused in air at 1500 °C for 24 h prior to quenching to a glass. A fourth composition composed of MIC99-8 powder doped with 1000 ppm Re standard solution and 1000 ppm Cl (added as NaCl) was also prepared in this fashion.

For the CMAS composition, reagent grade SiO_2, Al_2O_3, MgO and $CaCO_3$ were mixed and ground as noted above. The mixture was decarbonated at 1000 °C for 3 h and then fused at 1500 °C for 4 h prior to quenching to a glass. Quenched glasses were crushed, re-ground and re-melted three times to homogenize the major elements prior to adding 200 μl of a 1000 ppm Re standard solution before the fourth and final melt/quench cycle.

All final starting glasses were crushed and ground to a powder. The glass is nearly completely oxidized at 1500 °C in air over 24 h and, in the Fe-bearing compositions, most Fe is present as Fe^{3+} as reported in Table 1 (MIC99-8 $Fe^{3+}/Fe^{total} = 0.88$, WP-1 $Fe^{3+}/Fe^{total} = 0.79$). There is negligible Fe loss to the Pt crucible in an air atmosphere. Analyses of random chips of starting glasses indicate homogeneity in their major and trace element compositions (Table 1).

Powdered starting glass was loaded into 10 mm long 4 mm diameter Pt crucibles. For experiments in air, the crucible was held in a $4 \times 4 \times 3$ cm ceramic carrier and placed in the pre-heated box furnace. For experiments at more reducing conditions, the crucible was suspended in a Deltech DT-31-V-OT vertical tube gas-mixing furnace. The crucible was introduced to the gas-mixing atmosphere, the furnace sealed, and the desired fO_2 was achieved after approximately 5 min. Oxygen fugacities were imposed using CO–CO_2 gas mixtures at total gas flow rates of 200 SCCM, and continuously monitored using a solid zirconia electrolytic cell. Fluctuations in cell EMF were less than ±10 mV during each experiment corresponding to ±0.10 $\log fO_2$ units. Temperature was measured using a type S ($Pt/Pt_{90}Rh_{10}$) thermocouple immediately above the crucible. Temperature fluctuations were ±1 °C in the box furnace and ±3 °C in the gas-mixing furnace. Experiments for variable run durations were quenched in a stream of dry air (Table 2). After each experiment, the charges, composed entirely of quenched glass, were sectioned axially into two pieces. One half was mounted in epoxy, polished and examined in reflected light.

2.2. Analytical methods

2.2.1. Electron microprobe

Major and minor elements in the run products were determined using a CAMECA SX50 electron microprobe at the University of British Columbia at 15 kV acceleration voltage and a beam current of 20 nA with peak counting times of 30 s for Na, Mg, Al, Si, Ca, K, Ti, Cr, Mn, and Fe. Chlorine and sulphur contents were below detection (500 and 350 ppm, respectively) even with 300 s counting times at 10 kV acceleration voltage and a beam current of 50 nA. Major element profiles were collected perpendicular and parallel to the melt/gas interface as well as adjacent to the capsule walls (Fig. 2). Major element concentrations were homogenous throughout the entire charge.

2.2.2. Laser ablation-inductively coupled plasma-mass spectrometry (LA-ICP-MS)

Line profiles of trace element concentrations were collected perpendicular to the melt/gas interface by LA-ICP-MS at the University of Victoria using a VG Elemental PQ II S+ ICP-MS. Laser ablation was conducted using a Merchantek solid-state, frequency quadrupled 266 nm Nd:YAG UV laser pulsed at a frequency of 20 Hz with an energy of ~1.8 mJ. NIST 613 SRM glass containing 6.57 ppm Re (Sylvester and Eggins, 1997) was used as a standard. The spot size and line scan traverse rate were 20 μm and 0.008 mm/s, respectively. The detection limit for Re was 53 ppb. Data was collected in peak jumping mode with a dwell time of 10 ms at one point per peak. ^{43}Ca was used as the internal standard for NIST SRM and experimental run products. Each block of analyses consisted of measuring the NIST glass twice followed by <10 separate line scans before measuring the NIST glass twice again. Data are recorded as time resolved spectra in counts per second, collected over 360 s with 50 s allotted to collecting background concentrations. The spectra were then subdivided into 50 time slices, each representing ~50 μm of

Table 2
Summary table of run conditions and calculated D values for experiments obtained using the slopes from erf^{-1} versus distance from melt/gas interface demonstrated in Fig. 4

Composition	T	logfO_2	Duration (h)	logD_{Re}	Error*
MIC99-8	1300	−0.68	6	−7.1	0.1
MIC99-8	1300	−0.68	6	−7.2	0.1
MIC99-8	1300	−0.68	6	−7.2	0.1
MIC99-8	1300	−0.68	1	−7.0	0.3
MIC99-8	1300	−0.68	3	−7.3	0.2
MIC99-8	1250	−0.68	6	−7.6	0.2
MIC99-8	1250	−0.68	1	−7.7	0.2
MIC99-8	1350	−0.68	6	−6.7	0.1
MIC99-8	1350	−0.68	1	−6.8	0.2
MIC99-8 + Cl	1300	−0.68	6	−6.5	0.1
MIC99-8 + Cl	1300	−0.68	6	−6.6	0.1
MIC99-8 + Cl	1300	−0.68	3	−6.7	0.1
MIC99-8 + Cl	1300	−0.68	1	−6.4	0.2
MIC99-8	1300	−7.8	24	−7.8	0.1
MIC99-8	1300	−5.1	24	−7.5	0.1
MIC99-8	1300	−10	24	−7.8	0.2
MIC99-8	1300	−6	48	−7.8	0.2
MIC99-8	1300	−2	1	−7.5	0.2
MIC99-8	1300	−2	3	−7.3	0.1
WP-1	1300	−0.68	12	−8.7	0.2
WP-1	1300	−0.68	24	−8.4	0.1
WP-1	1250	−0.68	12	−8.5	0.2
WP-1	1250	−0.68	12	−8.4	0.1
WP-1	1350	−0.68	12	−7.9	0.1
WP-1	1350	−0.68	24	−8.0	0.1
CMAS	1300	−0.68	23	−7.6	0.1
CMAS	1300	−0.68	23	−7.5	0.1
CMAS	1300	−0.68	1	−7.4	0.2
CMAS	1300	−0.68	4	−7.4	0.2

* Errors calculated at 1σ for each experiment based on linear regression statistics of erf^{-1} versus distance from melt/gas interface.

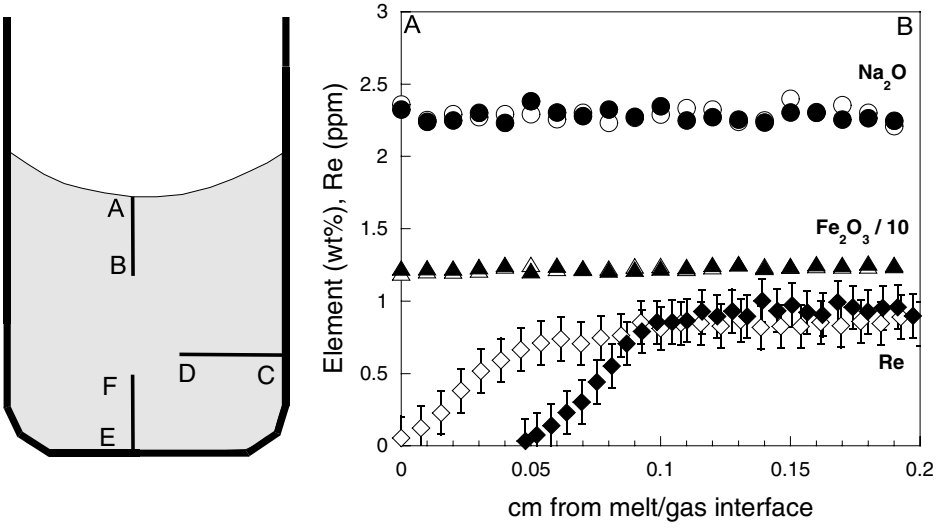

Fig. 2. Left: schematic drawing of an experimental run product and locations of line scans [ICPMS (Re, Yb), EMP (major elements)]. Charge diameter is 4 mm; height is 10 mm. Right: Rhenium and major element concentration profiles along transect (A–B) from melt/gas interface into glass. Rhenium profiles are shown for 6- (open diamonds) and 12-h runs (solid diamonds). Na_2O and Fe_2O_3/10 profiles are shown for the same 6- (open circles/triangles) and12-h runs (solid circles/triangles). Error bars for Re are calculated using 1σ counting statistics from ICPMS analysis. For Na_2O and Fe_2O_3 the size of symbols span the 1σ counting statistics from EMP analysis. No major element or Re concentration profiles were observed along transects (C–D) or (E–F).

scan length. The individual time slices were reduced to concentrations using the PlasmaLab© data reduction software.

Trace element concentration profiles were collected perpendicular to the melt/gas interface (Fig. 2) and at different locations along the interface. No distortions in the profiles by the presence of a meniscus at the glass/air interface were observed (Fig. 3). We conducted similar line scans across the charge into the Pt crucible walls and observed no change in Re concentration within the glass at or near this boundary. We therefore believe that Re diffusion was unidirectional to the melt/gas interface during the experiments. The thermal gradient along the length of our Pt crucibles is less than 1 °C as measured with a thermocouple. The Rayleigh number for the least viscous melt composition (MIC99-8) is less than 100 assuming planar geometry, a thickness of 1 cm and boundary conditions of $\Delta T = 1$ °C (Philpotts, 1990). The trivial thermal gradient and low Rayleigh number indicate that convection is negligible in our experimental design.

2.3. Data reduction

The volatility of Re from magma is a diffusion-controlled process limited by its diffusivity in silicate liquids (D_{Re}) and transport across a reacting interface (melt/gas). In practice, measuring D involves determining the actual transport distance and concentration gradients. The ideal experimental design generally is such that the sample can be treated as a one-dimensional, semi-infinite medium (Chakraborty, 1995). In the geometry of our experiments, which utilize open Pt crucibles, we assume the melt can be treated as a semi-infinite medium and the flux of species out the top as one-dimensional.

Crank (1975) derived mathematical relationships for diffusion in a one-dimensional, semi-infinite medium:

$$\frac{C - C_s}{C_o - C_s} = \mathrm{erf}\frac{x}{2\sqrt{(Dt)}} \quad (1)$$

The chemical gradient that serves as the driving force for chemical diffusion is quantified by the concentration term $(C - C_s/C_o - C_s)$ where C is the measured concentration along the profile, C_o is the initial concentration and $C_s$is the equilibrium surface concentration (Fig. 3). In the case of concentration-independent diffusion, the equation relating the diffusion coefficient (D), distance from the interface (x) and time (t) is:

$$x/(2\sqrt{Dt}) = \mathrm{erf}^{-1}(C - C_s/C_o - C_s) \quad (2)$$

where erf^{-1} is the inverse error function.

Plots of erf^{-1} $(C - C_s/C_o - C_s)$ versus the distance (x) from the melt/gas interface yield straight lines with slopes equal to $1/2\sqrt{Dt}$ (Fig. 4), from which D can be derived.

3. Results

The experimental results are summarized in Table 2 and plotted versus reciprocal temperature in Fig. 5. $\log D$ varies in a linear fashion with reciprocal T assuming there are no changes in Re speciation in silicate liquids with temperature. The temperature dependence of Re diffusion may be fitted to Arrhenius equations of the form:

$$\log D = \log D_0 - E_a/2.303RT \quad (3)$$

where D is the diffusivity at temperature T (K), D_0 is the pre-exponential or frequency factor, R is the gas constant and E_a is the activation energy for Re diffusion. The activation energies of Re diffusion are extracted from the slopes

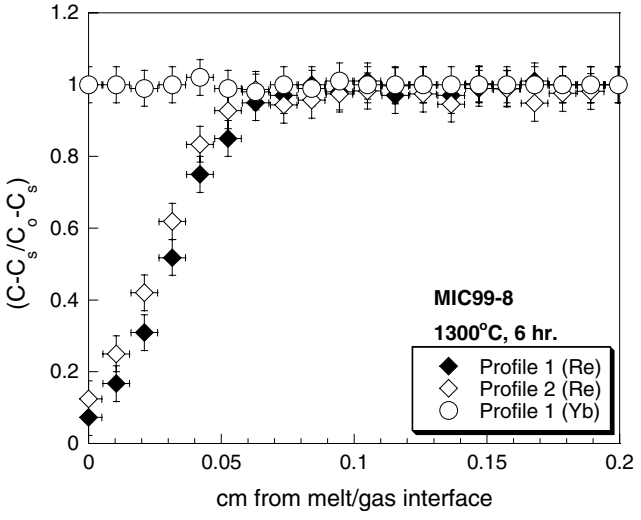

Fig. 3. Normalized Re and Yb concentration versus distance from the melt/gas interface measured at two positions normal to the melt/gas interface for basalt composition MIC99-8. $(C - C_s/C_o - C_s)$ error bars calculated at 1σ based on counting statistics. Distance error bars correspond to the scan distance for each time slice (~50 μm).

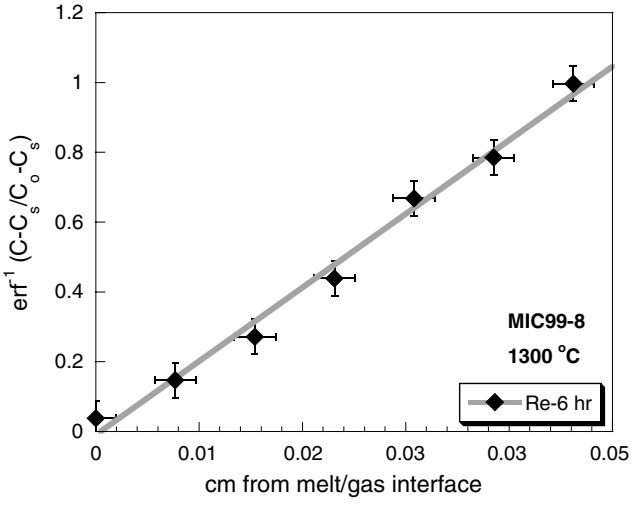

Fig. 4. Inverse error function (erf^{-1}) for normalized Re concentration $(C - C_s/C_o - C_s)$ versus distance from melt/gas interface for an experiment in basalt composition MIC99-8 shown in Fig. 3. Slope of line is equal to $1/2\sqrt{Dt}$ ($R^2 = 0.98$). $(C - C_s/C_o - C_s)$ error bars calculated at 1σ based on counting statistics. Distance error bars correspond to the scan distance for each time slice (~50 μm).

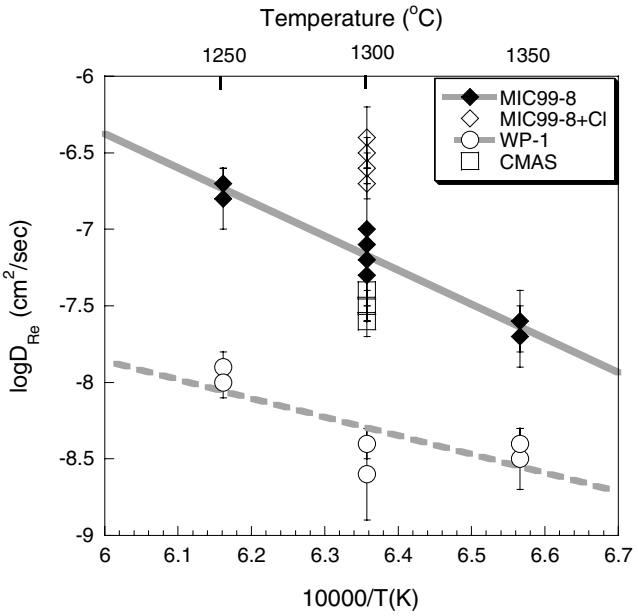

Fig. 5. Experimental data plotted as Arrhenius functions of absolute temperature. Error bars calculated at 1σ for each experiment based on linear regression statistics of erf^{-1} versus distance from melt/gas interface (Fig. 4 and Table 2).

of the lines in Fig. 5 and vary from 473 ± 4 kJ/mol in MIC99-8 melt to 202 ± 46 kJ/mol in WP-1 melt. The calculated frequency factors (D_0) for the basalt MIC99-8 is 8.5 ± 0.3 cm^2/s and -1.5 ± 4.1 cm^2/s for the dacite WP-1 composition.

In the basalt composition, runs conducted over 1-, 3- and 6-h durations show a Re concentration gradient that is well described using the D_{Re} values listed in Table 2. Over extended run durations (12–24 h) however, the shape and position of the Re concentration curves deviates strongly from our model calculations (Fig. 6). At a given temperature, the shape of the Re concentration curves are approximately uniform after 6 h, but the position of the curves (i.e., where Re concentration ~zero) is progressively displaced away from the melt/gas interface, leading to a region containing essentially no Re, that grows in thickness away from melt/gas interface with time.

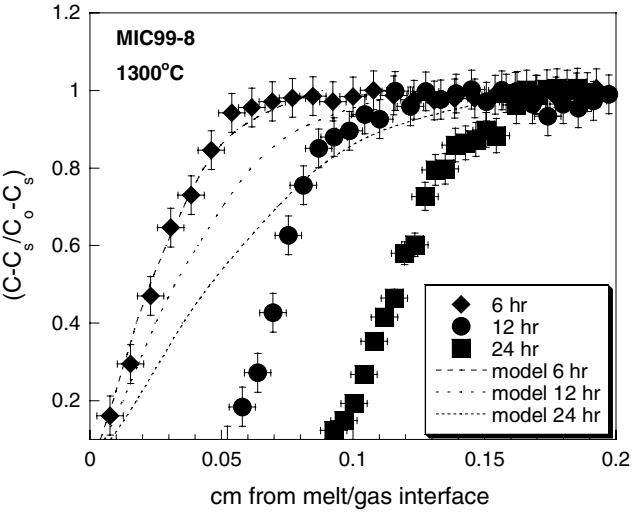

Fig. 6. Normalized Re concentration profiles for experiments performed in air as a function of run duration. Dashed lines are modeled diffusion curves [after Eq. (1)] using $\log D_{Re} = -7.2$ cm^2/s. Note the shape of the Re profile remains constant after 6 h, and the deviation of position of the curves relative to the model curves.

We are unaware of this phenomena being reported previously in any literature on diffusion or evaporation. Most importantly, this layer of Re depletion only occurs in the basaltic composition (MIC99-8) containing substantial Fe, and only under oxidizing conditions (i.e., $\log fO_2 > -2$) in experiments of over more than 6 h run duration. The layer of Re depletion does not develop in runs conducted at reducing conditions (i.e., $\log fO_2 < -2$), or in the CMAS and dacitic (WP-1) compositions. In the Fe-bearing dacite composition, we cannot rule out growth of the depletion zone over much longer times given the lower Re diffusivity in this composition. Initially, it might appear this moving interface in experiments performed in air is the well-known Stefan problem for moving boundary problems (i.e., Chebbi and Selim, 2006), but we emphasize it is not an actual physical movement of the melt/gas interface, only the shift in a chemical gradient away from that interface.

The causes of this Re depletion layer may include: (1) vigorous convection within this layer, (2) compositional change (Re, Na and/or Fe loss) within this layer or (3) oxidation of the melt near the melt/gas surface causing a change in melt structure or valence state of Re leading to increased Re diffusivity. Based on the calculated Rayleigh number for our experimental design, convection is not predicted. Furthermore, the CMAS composition has a viscosity similar to the MIC99-8 composition ($\log \eta = 2.32$ and 2.24, respectively) thus convection in a depleted layer would be the same for both compositions, yet a Re depletion layer only develops in the Fe-bearing one. A compositional change in or near the Re depletion layer is untenable, as we observe no change in Fe or Na loss near the melt/gas interface (Fig. 2) or the walls of the crucible either within or below the depleted layer.

As noted previously, all starting compositions were synthesized at 1500 °C. At these conditions, the Fe^{3+}/Fe^{total} in MIC99-8 calculated using the Kress and Carmichael (1988) algorithm is 0.88. At the lower T of our volatilization experiments in air, however, the equilibrium Fe^{3+}/Fe^{total} for MIC99-8 calculated using this algorithm is 0.98, requiring a slight amount of oxidation of the melt (increase in Fe^{3+}/Fe^{2+}). For this reason, we hypothesize that for experiments in air, higher valence states of Re in the melt are being reduced in the outermost layer to oxidize Fe^{2+} within this layer via a homogeneous equilibrium such as:

$$Re^{7+} + Fe^{2+} = Re^{6+} + Fe^{3+} \quad (4)$$

We suspect lower valence species of Re (i.e., Re^{6+}) diffuse faster than higher valence species Re^{7+}, and thus leaves a 'layer' impoverished with Re.

Although the growth of a zone of Re depletion near the melt/gas interface and the displacement of the Re concentration gradient away from this interface is puzzling, we emphasize its existence only in the oxidizing experiments on basalt conducted over more than 6 h. The Re depletion layer does not affect the outcome of our extracted D values, or the conclusions of our study.

3.1. Effect of composition

In one set of experiments, the MIC99-8 basalt powder was initially doped with Cl to a level of 1000 ppm, but analysis of this composition after synthesis showed it to contain Cl levels below detection (500 ppm). Preliminary results from Cl diffusion experiments in hawaiite melt ($\pm H_2O$) from Etna at 0.5 and 1.0 GPa and temperatures between 1250 and 1450 °C show $\log D_{Cl} = -4.8$ to -5.9 cm^2/s (Alletti et al., 2006). Because Cl is volatile, some was likely lost during synthesis and during the experiments but using the D_{Cl} values listed above, Cl would still be present albeit below detection. Nonetheless, the experiments conducted using the MIC99-8 composition doped with Cl yield a $\log D_{Re} = -6.6 \pm 0.3$ cm^2/s at 1300 °C (Table 2), almost an order of magnitude higher than that in the undoped composition at the same temperature ($\log D_{Re} = -7.2 \pm 0.3$ cm^2/s). The result indicates that Re diffusion is increased if Cl is present, even in trace amounts.

Experiments performed in the dacite (WP-1) and CMAS compositions at 1300 °C yield a $\log D_{Re}^{dacite} = -8.4 \pm 0.2$ cm^2/s and $\log D_{Re}^{CMAS} = -7.5 \pm 0.2$ cm^2/s (Table 2). Re diffusivity in dacite liquid is more than an order of magnitude lower than the corresponding basaltic composition at the same temperature whereas the basalt and CMAS compositions have similar diffusivities.

3.2. Effect of changing oxygen fugacity

Experiments were performed to examine Re diffusion under the range of fO_2 conditions characteristic of most natural magmas (Christie et al., 1986; Carmichael, 1991). In a set of experiments on MIC99-8 basalt, temperature and run duration were held constant at 1300 °C and 24 h, respectively, while fO_2 was varied between $\log fO_2 = -2$ to -10. At conditions near the fayalite–magnetite–quartz buffer (FMQ), $\log D_{Re}^{reducing} = -7.6 \pm 0.2$ cm^2/s, only slightly lower than D_{Re} for runs conducted in air ($\log D_{Re}^{air} = -7.2 \pm 0.2$ cm^2/s).. The value of $\log D_{Re}$ changes with fO_2 in a non-linear fashion (Fig. 7) and increases at fO_2 above the nickel–nickel oxide (NNO) buffer.

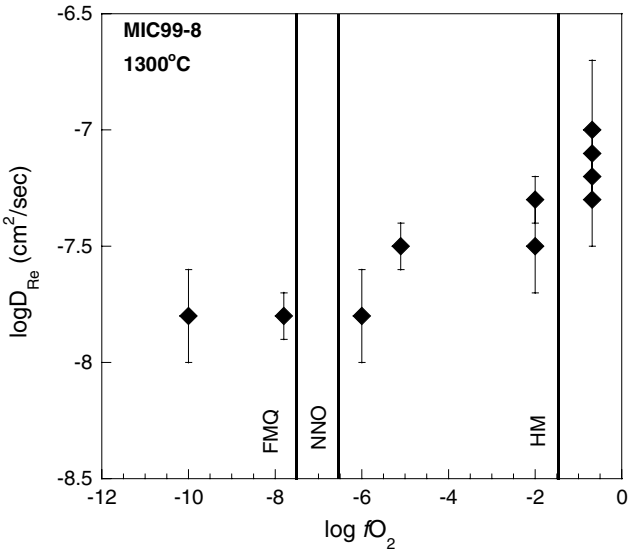

Fig. 7. $\log D_{Re}$ versus $\log fO_2$ for experiments on MIC99-8 (basalt) composition. Stippled lines mark the positions of the fayalite–magnetite–quartz (FMQ), Ni–NiO (NNO) and hematite–magnetite (HM) oxygen buffer assemblages calculated from Frost (1991). Note change in Re diffusivity at conditions above the NNO buffer. Error bars calculated at 1σ for each experiment based on linear regression statistics of erf^{-1} versus distance from melt/gas interface (Fig. 4 and Table 2).

4. Discussion

4.1. Re diffusion, volatization and speciation

At 1350 °C and 0.1 MPa, the diffusivity of Re in our basalt composition MIC99-8 is $\log D_{Re} = -6.7 \pm 0.2$ cm^2/s, not unlike CO_2 and Ar diffusivity in basalt at 500 MPa ($\log D_{CO_2, Ar} = -7.2$ and -6.6 cm^2/s, respectively, Nowak et al., 2004). If D_{Re} was orders of magnitude lower than that of other volatile constituents in magmas it would be difficult to ascribe to a model of Re degassing as a significant source for Re depletion in subaerially erupted magmas, because Re mobility would restrict transport of Re as a constituent to the melt/gas interface. The similar diffusivities of other volatile constituents and Re indicate there is no kinetic barrier for Re release as a volatile. Ultimately, the release of Re as a volatile is also dependent on its partition coefficient into the (C–H–S–Cl) gas phase, for which there is only empirical evidence from volcanic gas emissions, and currently no experimental constraints.

It has long been recognized that diffusivity is related to differences in melt structure, itself reflected in viscosity (i.e., Glasstone et al., 1941; Einstein, 1956), and sometimes described by the ratio of non-bridging oxygens to tetrahedral cations (NBO/T) in a melt composition (Mysen et al., 1982). In general, diffusivity decreases with increasing tetrahedral network formers (Si, Al) and decreasing network modifiers (Na, H_2O) (i.e., with decreasing NBO/T). Compared to our basalt and CMAS composition, dacite has a higher ratio of non-bridging oxygen to tetrahedral cations (NBO/T) and thus higher viscosity causing lower diffusivity of Re.

Diffusivity of an element may also change according to its speciation in the melt structure. Cotton and Wilkinson (1966) and Knacke et al. (1991) suggest that the species responsible for Re volatility from pure Re metal is Re_2O_7, suggesting a Re^{7+} valence state. Recently, Ertel et al. (2001) showed that the dominant oxidation state of

Re in silicate melts is Re^{6+}at fO_2 conditions below ~NNO. Our results show a measurable increase in D_{Re} above ~NNO (Fig. 7). Interestingly, Borisov and Jones (1999) also showed that evaporation of Re from pure Re wire at 1400 °C also increased at fO_2's greater than ~NNO. From these observations, we infer that Re^{6+} is the diffusing species at logfO_2's less than NNO, whereas Re^{7+} is the diffusing species at logfO_2's greater than this buffer.

Xiong and Wood (1999) showed that the dominant oxidation state in hydrothermal fluids was Re^{4+}, with Re present as a ReCl species. Carroll and Webster (1994) note that, similar to F, Cl may dissolve in melts as a metal chloride ($Me^{+}Cl$) species. It is unknown what metal species preferentially complex with Cl and to what extent but Fe and Na have been indicated as potential candidates.

Kiprianov and Karpukhina (2006) show volatile products above fluorine containing melts involve a $Me^{+}Cl$ species and include exotic species such as GeF_4. Given the uncertainty in Cl speciation, at 1300 °C, in our basaltic composition $\log D_{Re} = -7.2\ cm^2/s$ but this increased to $-6.6\ cm^2/s$ in Cl doped experiments, suggesting that the speciation and complexation of Re with Cl, even in trace amounts, significantly increases its diffusion and volatilization. In trace amounts, Cl is not expected to change the viscosity of the melt significantly (Dingwell and Hess, 1998) and thus melt viscosity is not a likely the cause for increased D_{Re} in experiments doped with Cl. Given the evidence above, we instead favor complexation of Re species with Cl species in silicate melts.

4.2. Application

Differences in Re contents of MORB, OIB and arc-type basalt may be related to the mechanism of degassing. Degassing of magma requires exsolution of constituents from the melt during de-pressurization. The process can occur as either a closed system (batch degassing) where gasses released by the magma remain in equilibrium with the liquid, or as an open system (fractional distillation) where gases exsolved from the magma are continuously lost from the system. Moreira and Sarda (2000) suggest that MORB and OIB experience different degassing mechanisms. They show noble gas ratios and isotopic compositions of MORB are best explained using a model of batch degassing, whereas a fractional distillation process best describes samples of OIB. This conclusion is challenged by Yamamoto and Burnard (2005) who argue that the He and Ar solubility ratio in MORB would have to be up to 15 times higher to account for the noble gas ratios using a batch degassing model. Alternatively, Burnard (1999), noting the correlation between vesicle size and its trapped volatiles (CO_2 and noble gases), showed that both MORB and OIB degassing can be modeled using a fractional distillation process (Yamamoto and Burnard, 2005). For the purpose of our discussion, we will assume that degassing of MORB, OIB and arc-type basalt results from an open system (fractional distillation) process.

Degassing of magmas occurs mostly within a magma chamber as pressure decreases and gas bubbles form. The most important volatile constituents in silicate magmas are H_2O and CO_2, with minor SO_3 and Cl (Jambon, 1994) all of which are likely to influence volatile release of Re from magma. Evaluating Re concentrations in subaerially versus subaqueously erupted magmas requires an estimate of the amount of degassing experienced in each case, which in a general way could be estimated by the volume percent of vesicles (vesicularity).

MORB's are typically erupted at depths of 2 km below sea level and generally have vesicularities of less than 5% by volume (Cashman and Mangan, 1994). In contrast, subaerially erupted arc-type basalts can have vesicularities approaching 60–70% depending on the mode of eruption (i.e., effusion) (Cashman and Mangan, 1994). Assuming Re depletion is related to gas loss, the Re abundances should scale with vesicularities. Unfortunately, there is no direct data on the vesicularity for each sample measured for its Re content (Fig. 1). The differences in vesicularities between subaqueously and subaerially erupted samples would suggest that Re abundances in the former are at least ten times greater than that of the latter. MORB and arc-type basalts have average Re concentrations of 0.956 and 0.233 ppb, respectively. Thus qualitatively, a general correlation between vesicularity and Re contents in basalts exists, but it must be used with caution, as vesicularity may not simply reflect volatile contents, rather degree of volatile supersaturation and magma ascent rate on vesicle formation and growth need also be considered.

Differences in Re contents among MORB, OIB and arc-type basalts may reflect differences in the source region and/or degrees of partial melting or fractional crystallization. The mineralogy (i.e., garnet presence) and presence of residual sulphide in the source region affect Re contents but these cannot fully account for the differences between all cases in Fig. 1 (Lassiter, 2003). For example, residual garnet in the source region of OIB and arc-type basalts could account for the lower Re contents in these rocks. However, Yb and Re are similarly compatible in garnet (Righter and Hauri, 1998) and thus, garnet in the source should act to deplete Yb as much as Re, which is not the case; Yb is not as depleted in OIB and arc-type basalts as in MORB (Lassiter, 2003). Additionally, among lavas from Kilauea, Re contents do not scale with indices of partial melting or fractional crystallization (Lassiter, 2003).

Several observations are suggestive that Re can be lost from magma as a volatile species. In arc volcanics from Aoba, Vanuatu, Re is enriched in olivine-hosted melt inclusions relative to their host magma (Sun et al., 2003b). Subaerially erupted basalts from Kilauea have lower Re contents than their submarine equivalents within the same volcanic pile (Lassiter, 2003). Re-rich mineral species are recognized at volcanic edifices (Korzhinsky et al., 1994; Taran et al., 1995). Because arc-type basalts are generally enriched in volatile components (0.2–6.1 wt% H_2O, 0–2100 ppm CO_2 and 500–2000 ppm Cl (Wallace, 2005))

relative to MORBs (0.1–0.5 wt% H_2O, 100–300 ppm CO_2 and <100 ppm Cl Dixon and Stopler (1995)) they likely experience more de-pressurization and gas production upon eruption, and potential Re loss as a volatile.

Re and Cl are strongly correlated in gas compositions measured from Kilauea (Crowe et al., 1987; Miller et al., 1990) suggesting the formation of a ReCl species may be important in Re loss during degassing. Our results confirm this suggestion, and clearly show that Re mobility is increased in the presence of Cl, even in trace amounts (<500 ppm). Cl contents of melt inclusions from arc-type basalts (typically 500–2000 ppm) are consistently higher than their MORB counterparts (<100 ppm) (Wallace, 2005) indicating greater Re loss via degassing from arc-type basalts compared to MORB.

Righter et al. (2002) argue that the low Re contents of arc-type basalts are the opposite that expected by Re behavior in fluids. The high solubility of Re in Cl-rich fluids (Xiong and Wood, 1999) suggest that arc-type magmas, which many believe to have formed by fluids that flux the mantle source region in subduction zones, should have high Re, yet data from arc basalts show the lowest Re concentrations. Given the increased Re diffusivity observed in Cl-bearing silicate liquids (Fig. 5 and Table 2), we hypothesize that the increased mobility and volatility of Re in Cl-bearing silicate liquids, coupled with the increased Cl content in arc-type basalts acts to deplete the magma of Re to a much greater extent than any Re enrichment associated with interaction of subduction-derived fluids to the source region of arc magmas.

Significant Re depletion from a lava flow having a thickness of meters would be impossible if it occurred exclusively through a diffusive process. Using the values of D_{Re} we obtain, the time for cooling and solidification of the lava (days) would greatly outpace the rate of diffusion required to deplete the lava (years). Rather, diffusion is only one part of the degassing process. The loss of Re as a volatile species from magma involves: (1) diffusion of Re to a melt/gas interface (gas bubble), (2) the partitioning (solubility) of Re into the gas/fluid phase, and (3) migration of the Re-bearing gas to a surface where it is released. The degree of degassing also depends on the amount of decompression (ascent rate) experienced by the magma. Our study sheds light on the first step in this process, but more experimental data are needed on the latter parts of the process.

5. Summary

Volatization experiments performed in basaltic, dacitic and CMAS melts at 0.1 MPa indicate that the diffusivity of Re is strongly affected by melt composition, and its speciation in the melt, and weakly affected by changes in fO_2. The negative correlation of vesicularities and Re concentrations in basalts erupted subaqueously and subaerially suggest that Re can be volatile and strongly partitioned into the gas phase. Re diffusivity in basalt is similar to that of CO_2 and Ar at 500 MPa (Nowak et al., 2004) suggesting no kinetic barrier to Re depletion by gas loss in subaerial eruptions. We therefore argue that Re depletion in basalts from intra plate and convergent margin tectonic settings does not require the presence of sulfide or garnet in the source regions of these magmas, but rather that Re can be lost as a volatile during ascent and emplacement.

Acknowledgments

We thank J. Spence and M. Raudsepp for their able assistance with ICPMS and EMP, respectively. Reviews by R. Linnen, A. Holzheid and an anonymous reviewer and discussions with L. Coogan helped improve the manuscript and are all greatly appreciated. This research was supported by a MAC Foundation Scholarship to JMM and NSERC of Canada Discovery Grant to D.C.

Associate editor: Brent T. Poe

References

Alard, O., Griffin, W.L., Pearson, N.J., Lorand, JP., O'Reilly, S.Y., 2002. New insights into the Re–Os systematics of sub-continental lithospheric mantle from in situ analysis of sulphides. *Earth Planet. Sci. Lett.* **203**, 651–663.

Alletti, M., Baker, D.R., Freda, C., 2006. Halogen diffusion in basaltic melt. *Geophys. Res. Abstr.* **8**, 05936.

Alves, S., Schiano, P., Allègre, C.J., 1999. Rhenium–osmium isotopic investigation of Java subduction zone lavas. *Earth Planet. Sci. Lett.* **168**, 65–77.

Alves, S., Schiano, P., Capmas, F., Allègre, C.J., 2002. Osmium isotope binary mixing arrays in arc volcanism. *Earth Planet. Sci. Lett.* **198**, 355–369.

Becker, H., 2000. Re–Os fractionation in eclogites and blueschists and the implications for recycling of oceanic crust into the mantle. *Earth Planet. Sci. Lett.* **177**, 287–300.

Bennett, V.C., Norman, M.D., Garcia, M.O., 2000. Rhenium and platinum group element abundances correlated with mantle source components in Hawaiian picrites: sulfides in the plume. *Earth Planet. Sci. Lett.* **183**, 513–526.

Borg, L.E., Brandon, A.D., Clynne, M.A., Walker, R.J., 2000. Re–Os isotopic systematics iof primitive lavas from the Lassen region of the Cascade arc, California. *Earth Planet. Sci. Lett.* **177**, 301–317.

Borisov, A., Jones, J.H., 1999. An evaluation of Re, as an alternative to Pt, for the 1 bar loop technique: an experimental study at 1400 °C. *Am. Mineral.* **84**, 1528–1534.

Brenan, J.M., McDonough, W.F., Dalpe, C., 2003. Experimental constraints on the partitioning of rhenium and some platinum-group elements between olivine and silicate melt. *Earth Planet. Sci. Lett.* **212**, 135–150.

Burnard, P., 1999. The bubble-by-bubble volatile evolution of two mid-ocean ridge basalts. *Earth Planet. Sci. Lett.* **174**, 199–211.

Carmichael, I.S.E., 1991. The redox states of basic and silicic magmas: a reflection of their source regions?. *Contrib. Mineral. Petrol.* **106** 129–141.

Carroll, M.R., Webster J.D., 1994. Solubilities of sulphur, noble gases, nitrogen, chlorine and fluorine in magmas. In: Carroll, M.R., Holloway, J.R. (Eds.), Volatiles in Magmas. Mineralogical Society of America. *Reviews in Mineralogy* 30, pp. 231–279.

Cashman, K.V., Mangan, M.T., 1994. Physical aspects of magmatic degassing II. Constraints on vesiculation processes from textural studies of eruptive products. In: Carroll, M.R., Holloway, J.R. (Eds.), Volatiles in Magmas. Mineralogical Society of America. *Reviews in Mineralogy* 30, pp. 447–479.

Chakraborty, S., 1995. Diffusion in silicate melts. In: Stebbins, J.F., McMillan, P.F., Dingwell, D.B. (Eds.), *Structure, Dynamics and*

Properties of Silicate Melts, Mineralogical Society of America 32, pp. 411–497.

Chebbi, R., Selim, M.S., 2006. The Stefan problem of evaporation of a volatile component from a binary liquid mixture. *J Heat Mass Transfer* **42**, 238–247.

Chesley, J., Ruiz, J., Righter, K., Ferrari, L., Gomez-Tuena, A., 2002. Source contamination versus assimilation: an example from the Trans-Mexican Volcanic Arc. *Earth Planet. Sci. Lett.* **195**, 211–221.

Christie, D.M., Carmichael, I.S.E., Langmuir, C.H., 1986. Oxidation states of mid-ocean ridge basalt glasses. *Earth Planet. Sci. Lett.* **79**, 397–411.

Cotton, F.A., Wilkinson, G., 1966. *Advanced Inorganic Chemistry: A Comprehensive Text*, second ed. Interscience, New York.

Crank, J., 1975. *The Mathematics of Diffusion*, second ed. Oxford University Press, USA.

Crowe, B.M., Finnegan, D.L., Zoller, W.H., Boynton, W., 1987. Trace element geochemistry of volcanic gases and particles from 1983 to 1984 eruptive episodes of Kilauea Volcano. *J. Geophys. Res.* **92**, 13708–13714.

Dingwell, D.B., Scarfe, C.M., 1985. Chemical diffusion of fluorine in melts in the system Na_2O–Al_2O_3–SiO_2. *Earth Planet. Sci. Lett.* **73**, 377–384.

Dingwell, D.B., Hess, K.-U., 1998. Melt viscosities in the system Na–Fe–Si–O–F–Cl: contrasting effects of F and Cl in alkaline melts. *Am. Mineral.* **83**, 1016–1029.

Dixon, J.E., Stopler, E.M., 1995. An experimental study of water and carbon dioxide solubilities in mid-ocean ridge basaltic liquids: Part 2. Applications to degassing. *J. Petrol.* **36**, 1633–1646.

Einstein, A. 1956. *Investigations on the Theory of Brownian Movement*. Dover.

Ertel, W., O'Neill, H.St.C., Sylvester, P.J., Dingwell, D.B., Spettel, B., 2001. The solubility of rhenium in silicate melts: implications for the geochemical properties of rhenium at high temperatures. *Geochim. Cosmochim. Acta* **65**, 2161–2170.

Frost, B.R., 1991. Introduction to oxygen fugacity and its petrologic importance. In: Lindsley, D.H. (Ed.), Oxide Minerals: Petrologic and Magnetic Significance. Mineralogical Society of America. *Reviews in Mineralogy* 25, pp. 1–9.

Glasstone, S., Laidler, K.J., Eyring, H., 1941. *The Theory of Rate Processes*. McGraw Hill, New York-London.

Hauri, E.H., Hart, S.R., 1997. Rhenium abundances and systematics in oceanic basalts. *Chem. Geol.* **139**, 185–205.

Hauri, E.H., Kurz, M.D., 1997. Melt migration and mantle chromatography, 2: a time-series Os isotope study of Mauna Loa volcano, Hawaii. *Earth Planet. Sci. Lett.* **153**, 21–36.

Jambon, A., 1994. Earth degassing and large scale geochemical cycling of volatile elements. In: Carroll, M.R., Holloway, J.R. (Eds.), Volatiles in Magmas. Mineralogical Society of America, *Reviews in Mineralogy* 30, pp. 479–517.

Kiprianov, A.A., Karpukhina, N.G., 2006. Oxyhalide silicate glasses. *Glass Phys. Chem.* **32**, 1–27.

, second ed.Knacke, O., Kubashewski, O., Hessekmann, K. (Eds.), 1991. *Thermochemical Data of Pure Substances*, Vols. I and II Springer, New York.

Korzhinsky, M.A., Tkachenko, S.I., Shmulovich, K.I., Taran, Y.A., Stienberg, G.S., 1994. Discovery of a pure rhenium mineral at Kudriavy volcano. *Nature* **369**, 51–52.

Kress, V.C., Carmichael, I.S.E., 1988. Stoichiometry of the iron oxidation reaction in silicate melts. *Am. Mineral.* **73**, 1267–1274.

Lassiter, J.C., 2003. Rhenium volatility in subaerial lavas: constraints from subaerial and submarine portions of the HSDP-2 Mauna Kea drillcore. *Earth Planet. Sci. Lett.* **214**, 311–325.

Lassiter, J.C., Hauri, E.H., 1998. Osmium-isotope variations in Hawaiian lavas evidence for recycled oceanic lithosphere in the Hawaiian plume. *Earth Planet. Sci. Lett.* **164**, 483–496.

Miller, T.L., Zoller, W.H., Crowe, B.M., Finnegan, D.L., 1990. Variations in trace metal and halogen ratios in magmatic gases through an eruptive cycle of the Pu'u O'o vent, Kilauea, Hawaii: July–August 1985. *J. Geophys. Res.* **95**, 12607–12615.

Moreira, M., Sarda, P., 2000. Noble gas constraints on degassing processes. *Earth Planet. Sci. Lett.* **176**, 375–386.

Mysen, B.O., Virgo, D., Seifert, F.A., 1982. The structure of silicate melts: implications for the chemical and physical properties of natural magmas. *Rev. Geophys. Space Phys.* **20**, 353–383.

Nowak, M., Schreen, D., Spickenbom, K., 2004. Argon and CO_2on the race track in silicate melts: a tool for the development of a CO_2 speciation and diffusion model. *Geochim. Cosmochim. Acta* **68**, 5127–5138.

Philpotts, A.R., 1990. *Principles of Igneous and Metamorphic Petrology*. Prentice Hall, Englewood Cliffs, New Jersey.

Righter, K., Hauri, E.K., 1998. Compatibility of Rhenium in garnet during mantle melting and magma genesis. *Science* **280**, 1737–1741.

Righter, K., Chesley, J.T., Ruiz, J., 2002. Genesis of primitive, arc-type basalt: constraints from Re, Os and Cl on depth of melting and role of fluids. *Geology* **30**, 619–622.

Roy-Barman, M., Allègre, C.J., 1994. $^{187}Os/^{186}Os$ ratios in mid-ocean ridge basalts and abyssal peridotites. *Geochim. Cosmochim. Acta* **58**, 5043–5054.

Schiano, P., Birck, J.-L., Allègre, C.J., 1997. Osmium–strontium–neodymium–lead isotopic covariations in mid-ocean ridge basalt glasses and the heterogeneity of the upper mantle. *Earth Planet. Sci. Lett.* **150**, 363–379.

Schiano, P., Burton, K.W., Dupré, B., Birck, J.-L., Guille, G., Allègre, C.J., 2001. Correlated Os–Pb–Nd–Sr isotopes in the Austral-Cook chain basalts: the nature of mantle components in plume sources. *Earth Planet. Sci. Lett.* **186**, 527–537.

Shirey, S.B., Walker, R.J., 1998. The Re–Os isotope system in cosmochemistry and high-temperature geochemistry. *Annu. Rev. Earth Planet. Sci.* **26**, 423–500.

Sun, W., Bennett, V.C., Eggins, S.M., Kamenetsky, V.S., Arculus, R.J., 2003a. Enhanced mantle-to-crust rhenium transfer in undegassed arc magmas. *Nature* **422**, 294–297.

Sun, W., Arculus, R.J., Bennett, V.C., Eggins, S.M., Binns, R.A., 2003b. Evidence for rhenium enrichment in the mantle wedge from submarine arc-like volcanic glasses (Paupa New Guinea). *Geology* **31**, 845–848.

Sylvester, P.J., Eggins, S.M., 1997. Analysis of Re, Au, Pd, Pt and Rh in NIST glass certified reference materials and natural basalt glasses by laser ablation ICP-MS. *J. Geostand. Geoanal.* **21**, 215–229.

Taran, Y.A., Hedenquist, J.W., Korzhinsky, M.A., Tkachenko, S.I., Shmulovich, K.I., 1995. Geochemistry of magmatic gasses from Kudryavy volcano, Iturup, Kuril Islands. *Geochim. Cosmochim. Acta* **59**, 1749–1761.

Wallace, P.J., 2005. Volatiles in subduction zone magmas: concentrations and fluxes based on melt inclusion and volcanic gas data. *J. Volcanol. Geotherm. Res.* **140**, 217–240.

Widom, E., Shirey, S.B., 1996. Os isotope systematics in the Azores: implications for mantle plume sources. *Earth Planet. Sci. Lett.* **142**, 451–465.

Woodhead, J., Brauns, M., 2004. Current limitations to the understanding of Re–Os behavior in subduction systems, with an example from New Britian. *Earth Planet. Sci. Lett.* **221**, 309–323.

Xiong, Y., Wood, S.A., 1999. Experimental determination of the solubility of ReO_2 and the dominant oxidation state of rhenium in hydrothermal solutions. *Chem. Geol.* **158**, 245–256.

Yamamoto, J., Burnard, P.G., 2005. Solubility controlled noble gas fractionation during magmatic degassing: implications for noble gas compositions of primary melts of OIB and MORB. *Geochim. Cosmochim. Acta* **69**, 727–734.